pH Dependence of the Reaction Catalyzed by Yeast Mg−Enolase†

Dmitriy A. Vinarov and Thomas Nowak*

Department of Chemistry and Biochemistry, University of Notre Dame, Notre Dame, Indiana 46556

Received May 6, 1998; Revised Manuscript Received August 12, 1998

ABSTRACT: The pH dependence of the chemical shifts of the ^{31}P resonances of enzyme-bound substrates 2-phosphoglycerate (PGA) and phosphoenolpyruvate (PEP) were measured to obtain further insight into the catalytic mechanism of yeast enolase. The ^{31}P resonances of PGA and PEP bound to the enolase−Mg complex are individually observed by NMR. The $K_{eq,internal} = 1.5$ favoring PEP was measured. A pH dependence of the ^{31}P chemical shifts gives pK_a values of 5.82 and 6.16 for bound PGA and PEP, respectively, indicating that both ligands bind predominantly with their phosphate groups as the dianionic species and their ionization has been altered. The phosphoryl group of PGA has been suggested as playing a role in catalysis [Nowak, T., Mildvan, A. S., and Kenyon, G. L. (1973) *Biochemistry 12*, 1690−1701]. The pH dependence of the kinetic parameters for Mg−enolase shows a single break in the plot of p$K_{m,PGA}$ vs pH at pH 6.27 with a pH independence above pH 7. This is consistent with the trianion of PGA preferably binding to the enzyme. The k_{cat} profile gives pK_A values of 5.94 and 8.35, and k_{cat}/K_m profiles give pK_A values of 5.85, 6.25, and 8.39. Activation studies with Mg^{2+} show a pH independence for the activator constant (K_a), but a pH-dependent inhibition at higher concentrations of Mg^{2+}. The log k_{cat} and k_{cat}/K_a profiles from Mg^{2+} activation give pK_A values of about 5.9 and 8.4. These results confirm the importance of residues with pK_A values of about 5.9 and 8.4 (His and Lys residues?) but do not support a function for the phosphoryl group of the substrate. The pH dependence of the $K_{i,Mg^{2+}}$ gives pK_A fits of 5.95, 7.13, and 8.35. Data from cation inhibition suggest that the phosphate of the substrate and a His residue on enolase may bind the inhibitory Mg^{2+}.

Yeast enolase (2-phospho-D-glycerate hydrolase, EC 4.2.1.11) catalyzes the reversible dehydration of D-2-phosphoglycerate (PGA)[1] to phosphoenolpyruvate (PEP) as a key step in both glycolysis and gluconeogenesis. The enzyme is a dimer of two identical subunits (*1*), with a subunit molecular mass of 46 500 Da (*2, 3*). Enolase has an absolute requirement for a divalent cation for enzymatic activity that can be fulfilled by variety of metal ions (*4*). The dehydration of PGA proceeds as a trans elimination reaction (*5*), via a carbanion intermediate, formed in a rate-limiting C-2 proton abstraction (*6, 7*). Subsequent steps involve sp^2 hybridization of the C-2 carbon and loss of the C-3 hydroxyl group. The resulting water molecule enters the coordination sphere of the metal ion at site I (*8*).

In the absence of substrate, there is a single metal-binding site for Mg^{2+} or Mn^{2+} per monomer of enolase. Metal binding at site I induces a conformational change at the active site and enables subsequent binding of the substrate (*9*). The metal ion at site I is believed to be directly involved in the catalytic process. Upon substrate binding, the second metal ion can bind at site II. The binding of Mn^{2+} to sites I and II of enolase in the presence of PGA shows little change over the pH range from 5.15 to 7.50 (*10*). This suggests that the ligands that bind cations at sites I and II are neither histidines, lysines, nor cysteine thiolates, but probably carboxylates from aspartate and/or glutamate and/or backbone carbonyl groups. The third, inhibitory, metal-binding site is titrated at a pH value of about 6.5−7.0 (*10*) and may be located either at a histidine-containing site, at the phosphoryl group of the substrate, or at both.

There are several catalytic mechanisms proposed for enolase, some of which have emerged from structural investigations of enolase from yeast (*11, 12*) and from lobster muscle (*16*). The identities of residues functioning in general acid−base catalysis are not yet established unambiguously. The crystal structure of yeast enolase, complexed with the equilibrium mixture of PGA and PEP (*11*), and a kinetic analysis of enolase mutants K345A, E168Q, and E211Q (*13*) were interpreted as Lys 345 being the likely candidate for a catalytic base. The Glu211 was assigned the role of proton donor to the leaving hydroxyl group in the forward reaction and as an activator of the water molecule in the reverse reaction. An argument in favor of Glu211−Lys345 as the catalytic acid−base pair is based on the results of Rose and co-workers (*5*) who determined that the enolase-catalyzed elimination of water from PGA proceeds via antistereochemistry. Any group(s) assisting in the leaving of the C-3 hydroxyl group should be found on the side of the substrate

† The research reported in this paper was supported by a research grant from the National Institute of Health (DK 17049) to T.N.

* To whom correspondence should be addressed. Phone: (219) 631-5859. Fax: (219) 631-3567. E-mail: Nowak.1@nd.edu.

[1] Abbreviations: PAH, phosphonoacetohydroxamate; PEP, phosphoenolpyruvate; PGA, D-2-phosphoglycerate; PRR, water proton longitudinal relaxation rate; EPR, electron paramagnetic resonance; NMR, nuclear magnetic resonance; HEPES, *N*-(2-hydroxyethyl)-piperazine-*N*′-2-ethanesulfonic acid; MES, 2-(*N*-morpholino)ethanesulfonic acid; TRIS, 2-amino-2-hydroxymethyl-1,3-propanediol; TAPS, *N*-[tris(hydroxymethyl)-methyl]-3-aminopropanesulfonic acid; SDS, sodium dodecyl sulfate.

10.1021/bi981047o CCC: $15.00
Published on Web 10/07/1998

opposite to the catalytic base. Lys345 and Glu211 are located on the opposite sides of the substrate.

Chemical modification studies have shown that complete inactivation of enolase by diethyl pyrocarbonate correlates with the modification of the 6 histidyl residues/subunit. The presence of substrate or substrate analogue 3-phosphoglycerate, plus an excess of Mg^{2+}, protects 2 histidyl residues/subunit from modification. Although such protection could arise from a number of causes, the likelihood exists that two histidyl residues are present at the active site of enolase and may be involved in catalysis and/or binding of the third, inhibitory, Mg^{2+}. All of the available crystal structures of enolase show that there are two histidyl residues at the active site, His159 and His373. His159 is located 3.0 Å from the C-2 proton of PGA and could play a key role in the initial step of the reaction. His373 is positioned at the C-3 hydroxyl group of the substrate and could be involved in the departure of the leaving group (*14, 11, 15*).

On the basis of the hypothesis explaining the function of metal I developed by Nowak et al. (*8*) and modified by Brewer (*16*), the phosphoryl group of the enzyme-bound substrate has been suggested as playing a role in catalysis. There is a putative interaction between a molecule of metal-bound water and the phosphoryl group of the substrate/product. Catalysis involves transfer of protons to and from the metal-bound water molecule, and the phosphate of the substrate. The proton from C-2 adds to a metal-bound water molecule while the proton that bridges the metal I-bound hydroxy methyl group and the phosphate group of the substrate is transferred to the metal-hydroxyl. The phosphate putatively acts as a base to deprotonate the water molecule. To gain a greater understanding of the possible role played by the phosphoryl group, it is desirable to know the ionization state of this group on the enzyme-bound substrate. If the phosphate is directly involved in enolase catalysis, its ionization should affect catalysis.

Enolase was shown to be the target enzyme for the inhibition of glycolysis by fluoride ion (*17*). Inhibition of enolase by F^- itself is quite weak. In the presence of P_i, an intracellular physiological buffer, inhibition of Mg^{2+} activated enzyme by F^- becomes extremely potent. Binding data indicate a random addition of F^- and P_i to the enzyme−metal complex to produce an inactive enolase species (*18*). It is believed that the structure of the inhibitory complex is analogous to the proposed catalytic complex and may be analogous in structure to the transition state of the reaction.

The purpose of this study is to characterize the enzyme−substrate interactions of yeast enolase involving ionizable groups that might play a role in binding and/or catalysis. The ionization state of inorganic phosphate in the highly inhibitory, slowly exchanging enolase−Mn^{2+}−F^-−P_i complex is determined using ^{31}P NMR. The ^{31}P chemical shifts for the enolase−Mn^{2+}−(PGA−PEP) complex are analyzed as a function of pH. These interactions can be characterized using steady-state kinetic pH profile studies. An analysis of the pH variation of the kinetic parameters K_m, k_{cat}, and k_{cat}/K_m for substrates and K_i for inhibitors can allow the identification of functionally important ionizable groups, their apparent pK_A values, preferred ionization states, and their possible roles in binding and/or catalysis.

EXPERIMENTAL PROCEDURES

Enolase Purification. PGA, MES, HEPES, and TAPS were purchased from Sigma (St. Louis, MO). All other reagents were of the highest purity available. Solutions were prepared in distilled, deionized water.

Enolase was purified from Baker's yeast using a revised procedure developed in our laboratory (*19*) that yields enzyme with a specific activity of 120 units/mg measured under standard conditions (see below). This enzyme shows a single band of protein corresponding to the molecular mass of 46 500 Da on SDS−polyacrylamide gel electrophoresis and a single peak on a capillary electrophoresis. Purified enolase was stored as a lyophilized powder at −20 °C.

Enolase Assay. Enolase was prepared prior to experimentation by dissolving the dry powder in a minimal amount of the appropriate buffer and passing the solutions through a G-25 column (1 × 14 cm) that contained 2 cm of Chelex-100 on the top. The column was equilibrated with 50 mM appropriate buffer. The pH dependence studies of the activation of the enzyme by Mg^{2+} were performed at saturating concentrations of PGA (2 mM). The pH dependence of the velocity response to PGA concentrations was analyzed at Mg^{2+} concentrations that were optimal prior to the onset of the cation inhibition (1 mM).

The enzyme was normally assayed by a modification of the method described previously (*20*). The typical assay mixture contains 50 mM HEPES, pH 7.5, 50 mM KCl, 2 mM PGA, and 1 mM $MgCl_2$ in a volume of 1 mL. The increase in absorbance due to the formation of the product, PEP, was measured at 230 nm on a Gilford 240 spectrophotometer. The enzyme concentrations were determined by using the extinction coefficient at 280 nm of 0.89 mL mg^{-1} cm^{-1} (*38*) and a molecular weight of 93 000/dimer (*3*). The specific activity was initially determined as the change in absorbance at 230 nm/min divided by the enzyme concentration expressed as absorbance units at 280 nm (*21*). Data are reported as specific activity in standard activity units of micromoles of product produced per milliliter per minute per milligram. A unit of activity at 230 nm [$(\Delta A_{230}/A_{280})$-min^{-1}] corresponds to 0.32 units/mg at pH 7.5 and above. Velocity data were properly normalized by measuring the extinction coefficient for PEP over the pH range where kinetic studies were performed.

UV Difference Spectroscopy. UV difference spectra were obtained with a Beckman DU-40 spectrophotometer. Difference spectra were measured from 240 to 320 nm. Routinely, 1 mL sample solutions containing 25 μM enolase (50 μM sites), 1 mM $MgCl_2$, 50 mM Tris−HCl, pH 7.5, and 50 mM KCl were titrated with microliter quantities of ligand solutions. Corrections were made in ΔA for dilution of the enzyme from the original concentration of 50 μM sites.

^{31}P-NMR Spectroscopy. The ^{31}P-NMR spectra were obtained on a Varian VXR500 spectrometer equipped with a 5 mm variable frequency probe and operating at a Larmor frequency of 202.4 MHz, using a spectral width of 20 kHz at 21 °C. Twenty percent D_2O was added to the buffer for setting the field/frequency lock. An external standard of 85% H_3PO_4 was used for setting 0 ppm and for analyzing line broadening.

Data Analysis. The dissociation constants for substrate binding from UV difference titrations were obtained by fitting

the data to the expression

$$\Delta A/\Delta A_{max} = \{K_d + [E]_t + [L]_t - \{K_d^2 + [E]_t^2 + [L]_t^2 + 2K_d([E]_t + [L]_t) - 2[E]_t[L]_t^{1/2}\}\}/2[E]_t \quad (1)$$

where ΔA is the corrected change in absorbance induced by ligand binding at total ligand concentration $[L]_t$ and at total enzyme concentration $[E]_t$ (*18*). The ΔA_{max} is the change in absorbance obtained by extrapolation to infinite ligand concentration.

Titration parameters from the ^{31}P-NMR experiments were obtained by nonlinear least-squares fits of the one-proton titration curve

$$\delta_{(pH)} = (\delta_{HA} + \delta_{A-}10^{pH-pK_a})/(1 + 10^{pH-pK_a}) \quad (2)$$

of the experimental chemical shift, $\delta_{(pH)}$, where δ_{HA} is the chemical shift in the acidic pH limit, and δ_{A-} represents the chemical shift in the basic pH limit (*22*).

Steady-state reaction rates were determined by measuring the slope of a line drawn tangent to the reaction progress curve. The initial velocity data obtained at each pH were then best fit to the Michaelis−Menten equation

$$v/V_{max} = 1/(1 + K_m/[S]) \quad (3)$$

for the determination of the apparent Michaelis constants (K_m) and maximal velocity (V_{max}). All data were corrected for the effect of pH on the molar extinction coefficient of PEP at 230 nm in the standard assay mixture.

In the pH range 6.4−9.2, the kinetic data for the activation by Mg^{2+} was also best fit to the equation for uncompetitive substrate inhibition equation

$$v/V_{max} = 1/(1 + K_m/[S] + [S]/K_i) \quad (4)$$

where K_i is the inhibition constant for binding of Mg^{2+} at the inhibitory site, site III.

The variation of values for K_m as a function of pH were best fitted to the log form of eq 5:

$$Y = C/(1 + [H^+]/K_A) \quad (5)$$

The variation of values for k_{cat} as a function of pH were best fitted to the log form of eq 6:

$$Y = C/(1 + [H^+]/K_A^{ES} + K_B^{ES}/[H^+]) \quad (6)$$

The variation of values for k_{cat}/K_m or K_i as a function of pH were best fitted to the log form of eq 7:

$$Y = C/\{[(1 + [H^+]/K_A^E + [H^+][H^+])/K_A^E K_B^E] + K_C^E/[H^+]\} \quad (7)$$

In eqs 5−7, Y represents the value of K_m, k_{cat}, k_{cat}/K_m, or K_i at a particular pH value; C represents the pH-independent value of the corresponding parameter; K_A^{ES} and K_B^{ES} are the equilibrium constants for two ionizable groups in the enzyme−substrate complex, K_A^E, K_B^E, and K_C^E are the equilibrium constants for ionizable groups in the free enzyme or substrate, and H^+ is the hydrogen ion concentration.

Data were best fitted by either the nonlinear least-squares fitting program, EZ-FIT (*23*) or Table Curve 2D (Jandel Scientific). The EZ-FIT program uses the Nelder−Mead simplex and Marquardt nonlinear regression algorithms and includes model discrimination parameters based on the Student *t*-test. The Table Curve 2D program uses the Levenburg−Marquardt procedure for finding the global minimum of the squared sum of deviations.

RESULTS

Ionization State of the Phosphate Groups of Substrates and P_i Bound to Enolase−Mg^{2+}. UV difference spectroscopy indicates small changes in extinction coefficient of enolase−Mg upon ligand binding. The UV difference spectroscopic titrations reveal that the presence of F^- greatly increases the affinity of P_i for the enolase−Mg^{2+} complex. These titrations result in the formation of a tightly bound enolase−Mg^{2+}−F^-−P_i quaternary complex. The presence of 10 mM F^- decreases the apparent K_d of P_i for enolase−Mg from $K_d = 640 \pm 10$ μM to $K_d = 5.67 \pm 0.05$ μM (data not shown). The tight binding of P_i to form the quaternary enolase−Mg−F^-−P_i complex can allow spectra of bound P_i in this complex to be observed. The standard titration curves of the ^{31}P chemical shift of P_i in the pH range 5.5−8.5 for the P_i, P_i−Mg^{2+}, and P_i−Mg^{2+}−F^- complexes and the pH dependence of the ^{31}P chemical shift for the enolase−Mg^{2+}−F^-−P_i complex were measured at 202.4 MHz (Figure 1). The titration parameters were obtained by nonlinear least-squares best fits of the one-proton titration curves of the chemical shift and the results are summarized in Table 1. In the pH range 5.4−7.5, inorganic phosphate in the enolase−Mg^{2+}−P_i−F^- complex ionizes and its behavior is similar to that of P_i in solution.

The ^{31}P chemical shifts for the enolase−Mg^{2+}-(PGA−PEP) complex have been analyzed as a function of pH. The ^{31}P spectrum for PGA in the presence of excess enolase sites and saturating Mg^{2+} was obtained. Two resonances corresponding to the phosphate group of PGA and PEP are observed (Figure 2A). The exchange rate between the substrate (PGA) and product (PEP) bound to the enzyme must be slow on the NMR time scale. To clearly assign the observed resonances for the enzyme-bound PGA and PEP the ^{1}H-coupled spectrum of the enolase−(PGA−PEP) complex was obtained. The resonance appearing further downfield (4.80 ppm) shows a doublet due to ^{1}H coupling between the phosphorus and the C-2 proton of PGA (Figure 2B). This resonance is assigned to PGA. No long-range ^{1}H coupling is observed for the resonance at 3.03 ppm leading to its assignment as PEP. The pH dependence of the chemical shifts for free PGA and PEP in solution were performed (Figure 3, panels A and B) and the pK_A values calculated (Table 1). The ionization state of the phosphates of enzyme-bound PGA and PEP were determined by a pH dependence of the chemical shifts for the enzyme-bound substrates (Figure 3, panels c and d) and the pK_A values are summarized in Table 1.

The results indicate that at pH 7.5−7.75 both substrates (PGA and PEP) bind to enolase−Mg with this phosphate group as the dianionic species. Enzyme-bound PGA and PEP are characterized by an increased shielding as reflected in an upfield chemical shift for both species, relative to free PGA and PEP. The $K_{eq,internal} = 1.5$ favoring PEP and is determined by an integration of the two resonances. The $K_{eq,internal}$ is pH independent.

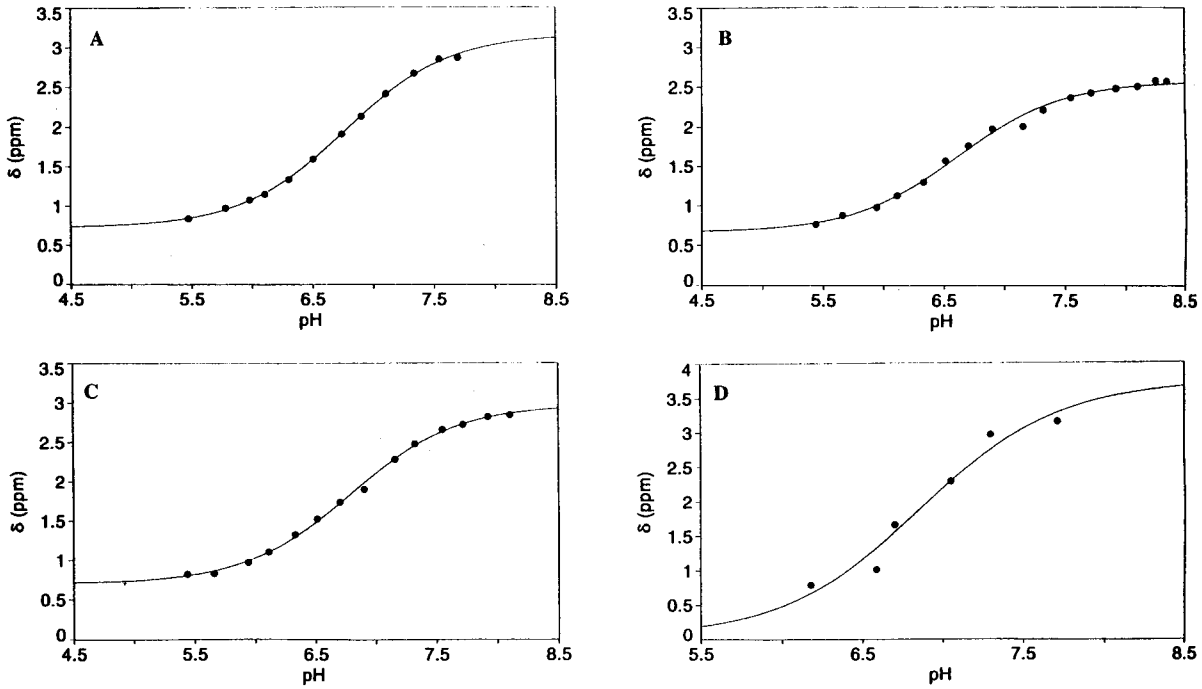

FIGURE 1: The pH dependence of the ^{31}P chemical shift of P_i and several P_i complexes. The ^{31}P chemical shift (δ) of P_i was measured for various inorganic complexes. The ^{31}P spectra were obtained at 202.4 MHz on a Varian VXR500 NMR spectrometer using quadrature phase detection in a Fourier transform mode. Twenty percent D_2O was added to the buffer for field/frequency lock. An external standard of 85% H_3PO_4 was used to set zero ppm and to analyze line broadening. Titration parameters were obtained by nonlinear least-squares fits of the one-proton titration curve (eq 2). (A) The pH dependence of δ for P_i: $[P_i] = 1$ mM; $[KCl] = 50$ mM. (B) The pH dependence of δ for P_i-Mg^{2+}: $[P_i] = 1$ mM; $[Mg^{2+}] = 10$ mM; $[KCl] = 50$ mM. (C) The pH dependence of δ for $P_i-Mg^{2+}-F^-$: $[P_i] = 1$ mM; $[Mg^{2+}] = 10$ mM; $[F^-] = 50$ mM; $[KCl] = 50$ mM. (D) The pH dependence of δ for enolase-$P_i-Mg^{2+}-F^-$: [Eno] = 2 mM sites; $[Mg^{2+}] = 4$ mM; $[P_i] = 1$ mM; $[F^-] = 50$ mM; $[KCl] = 50$ mM.

Table 1: Henderson−Hasselbach Fit for the ^{31}P-NMR Titration Curves[a]

complex	pK_A value	chemical shift (ppm) $\delta_{(HA)}$	chemical shift (ppm) $\delta_{(A-)}$
P_i	6.62 ± 0.07	0.70 ± 0.02	2.70 ± 0.05
$Mg^{2+}-P_i$	6.76 ± 0.07	0.75 ± 0.05	2.90 ± 0.02
$Mg^{2+}-P_i-F^-$	6.78 ± 0.05	0.70 ± 0.01	2.90 ± 0.02
Eno−$Mg^{2+}-P_i-F^-$	6.85 ± 0.16	0.30 ± 0.10	3.50 ± 0.10
PGA	6.86 ± 0.15	1.40 ± 0.10	4.20 ± 0.10
PEP	6.62 ± 0.17	−3.00 ± 0.10	0.50 ± 0.05
Eno−Mg^{2+}−PGA	5.82 ± 0.05	1.30 ± 0.10	5.00 ± 0.20
Eno−Mg^{2+}−PEP	6.16 ± 0.05	0.70 ± 0.10	3.50 ± 0.10

[a] Titration data were fit to eq 2.

Buffer Effects on the Steady-State Kinetic Parameters. The first step in a pH study is to determine a suitable set of buffers to cover the pH range of interest. Buffers can be switched from one to another over the pH range, or a mixture of buffers can be used in which each component covers a different portion of the pH profile. Overlaps of the steady-state kinetic parameters must be established when different buffers are used for various portions of the pH profile and buffers used for overlapping should not have pK_A values more than 1.5 to 2 units apart.

Several buffers were tested over a variety of pH ranges for their effects on steady-state kinetic parameters of the enolase catalyzed reaction. In the pH range 5.4−6.5, MES (pK = 5.9) was used; in the pH range 6.5−8.0, HEPES (pK = 7.3) was used; and in the pH range 8.0−9.2 TAPS (pK = 8.2) was used. The steady-state kinetic parameters of yeast enolase, determined using all three buffers at overlapping pH values, were identical within experimental error. Negligible buffer effects on the steady-state kinetic parameters for Mg^{2+} and PGA on enolase activity in the pH range 5.4−9.2 are shown in Table 2. The steady-state kinetic data were corrected for pH effects on the extinction coefficient of PEP at 230 nm.

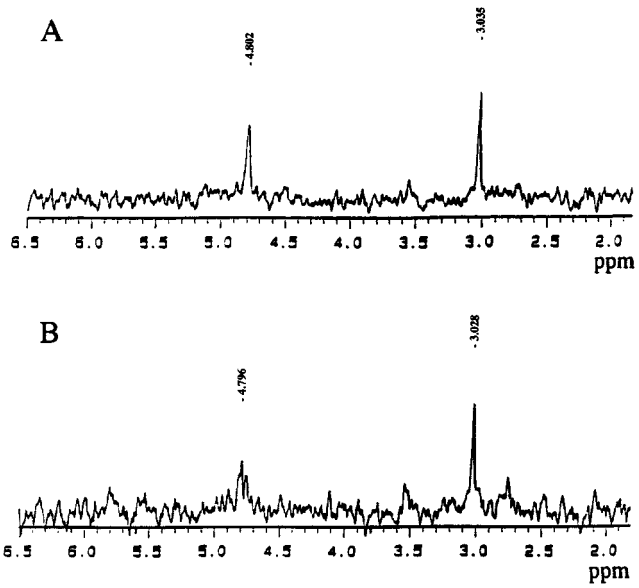

FIGURE 2: The ^{31}P spectrum of the enolase−Mg^{2+}-(PGA−PEP) complex. Spectra were obtained at 21 °C with 1200 scans. [Eno] = 2 mM sites, $[Mg^{2+}] = 2$ mM, [PGA]+[PEP] = 1 mM, [Hepes] = 50 mM, pH = 7.5, 20% D_2O. The resonance at 4.80 ppm is the phosphorus of enzyme-bound PGA and the resonance at 3.03 ppm is the phosphorus of enzyme-bound PEP. (A) The ^1H decoupled spectrum. (B) The ^1H coupled spectrum.

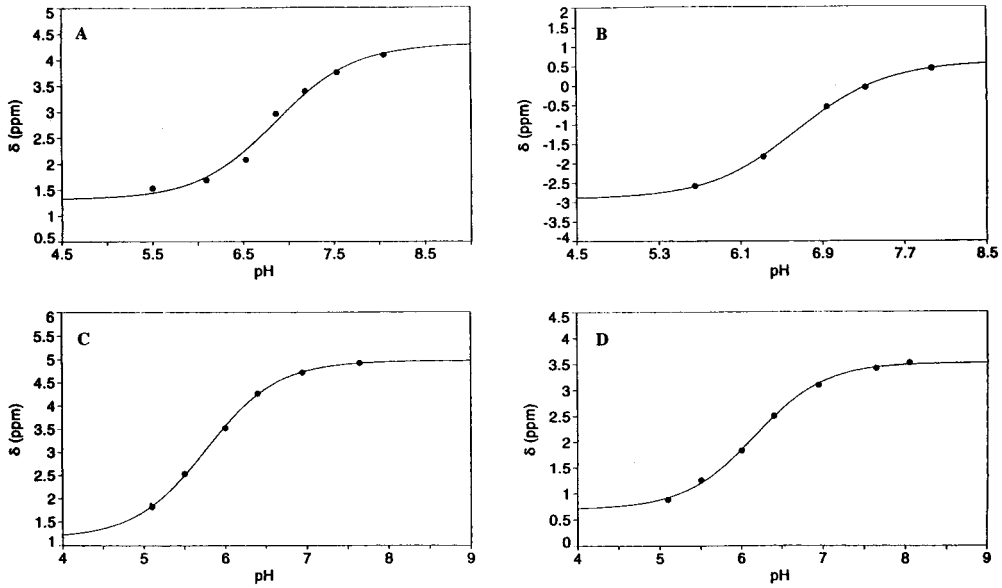

FIGURE 3: The pH titration curves of the ^{31}P chemical shift of PGA and PEP. The ^{31}P chemical shifts of free PGA and PEP and for the enolase−Mg−(PGA−PEP) complex were measured as a function of pH. (A) The pH dependence of δ for PGA: [PGA] = 10 mM. (B) The pH dependence of δ for PEP: [PEP] = 10 mM. (C) The pH dependence of δ for PGA in the enolase−Mg−(PGA−PEP) complex: [Eno] = 2 mM sites; [PGA] + [PEP] = 1 mM; [Mg^{2+}] = 2 mM; [KCl] = 50 mM; [MES] or [Hepes] = 50 mM. (D) The pH dependence of δ for PEP in the enolase−Mg−(PGA−PEP) complex: same experiment as panel C.

Table 2: Buffer Effects on the Steady-State Kinetic Parameters for Mg^{2+} and for PGA with Yeast Enolase[a]

buffer	pH	SA, Mg^{2+} † (units/mg)	K_A, Mg^{2+} † (μM)	$K_{i,Mg^{2+}}$ † (mM)	$K_{m,PGA}$‡ (μM)	SA, PGA‡ (units/mg)	$K_{m,PGA}$§ (μM)	SA, PGA§ (units/mg)
Mes	5.43	60.1	20.9		350.8	44.0	264.0	29.9
Mes	5.75	93.1	21.8		210.0	61.9	160.9	40.7
Mes	5.97	97.9	22.1		100.0	113.4	79.8	49.7
Mes	6.24	112.7	21.8	24.5	70.5	115.9	58.7	57.9
Hepes	6.24	111.1	21.5	26.4	70.1	116.5	58.5	58.4
Mes	6.54	117.2	22.0	11.8	55.0	114.2	42.9	68.1
Hepes	6.52	116.2	22.0	12.9	50.4	113.7	42.8	67.3
Mes	6.73	117.7	21.5	7.9	40.3	106.5	35.5	66.8
Hepes	6.74	118.1	21.8	8.3	40.5	107.5	34.6	67.1
Hepes	7.26	118.9	22.0	3.7	35.6	91.2	32.0	57.6
Hepes	7.37	114.9	22.2	2.9	31.6	89.1	27.8	57.4
Hepes	7.54	111.5	21.7	2.5	32.9	86.8	29.2	58.9
Hepes	7.78	109.5	21.6	2.6	32.5	78.1	32.4	56.1
Taps	7.81	108.3	21.4	2.7	33.5	79.4	31.5	56.3
Hepes	8.02	96.7	20.9	2.9	30.8	74.2	31.5	50.2
Hepes	8.29	87.4	20.5	3.5	30.2	63.7	28.5	44.3
Hepes	8.51	79.0	22.0	4.9	31.6	46.4	27.9	38.7
Taps	8.54	78.8	20.8	5.2	35.0	47.1	30.0	37.6
Taps	8.75	64.9	21.9	6.4	36.2	32.5	29.5	27.7
Taps	9.00	43.7	20.4	8.8	30.5	23.5	30.1	18.5
Taps	9.25	29.5	21.3	16.2	34.0	9.8	27.6	11.1

[a] The kinetic parameters were determined under conditions where yeast enolase was saturated with 2 mM PGA (†), saturated with 1 mM Mg^{2+} (‡), and in the presence of inhibitory concentrations of Mg^{2+} (§). The reaction mixture also contained 50 mM KCl and 50 mM buffer. Steady-state velocity data were fit to the Michaelis−Menten equation: $v/V_{max} = 1/(1 + K_m/[S])$ for the determination of the apparent Michaelis constants (K_m) and maximal velocity (V_{max}) and to the equation for uncompetitive substrate inhibition: $v/V_{max} = 1/(1 + K_m/[S] + [S]/K_i)$, for the determination of K_i for the binding of Mg^{2+} at site III. The parameters determined from the equation that best-fit the data are shown. The experimental error was within 7%.

pH Effects on the Steady-State Kinetic Parameters with Mg^{2+} as a Variable. The steady-state kinetic parameters for the activation of yeast enolase by Mg^{2+} were determined as a function of pH. The apparent K_A and k_{cat} values with Mg^{2+}, designated $K_{A,app}$ and $k_{cat,app}$, were determined over the pH range 5.4−9.25. Activation studies with Mg^{2+} show a pH independence for the activator constant (K_a) (data not shown). The k_{cat} and k_{cat}/K_A profiles (Figure 4, panels A and B) do not differ considerably from one another. Both k_{cat} and k_{cat}/K_A profiles are bell-shaped and illustrate the decrease in the rate of the reaction at both high and low pH values. The fit of the k_{cat} data to eq 6 yielded pK_A values of 5.84 ± 0.06 and 8.55 ± 0.03 with a $k_{cat,max}$ of 113.5 ± 2.8 s^{-1}. The k_{cat}/K_a profile gave the pK_A of the acidic group of 5.93 ± 0.06 and the pK_A of the basic group of 8.39 ± 0.03. These values are similar to pK_A values in the k_{cat} profile. At higher concentrations of Mg^{2+} the pH-dependent inhibition is observed (Figure 4c). The change in the K_i values of Mg^{2+} as a function of pH gave rise to a bell-shaped K_i profile with a limiting slope of +2 on the acid side and −1 on the alkaline side (Figure 4c). Fitting the data to eq 7 yielded pK_A values of 5.95 ± 0.20, 7.13 ± 0.08, and 8.35 ± 0.05 and a value of

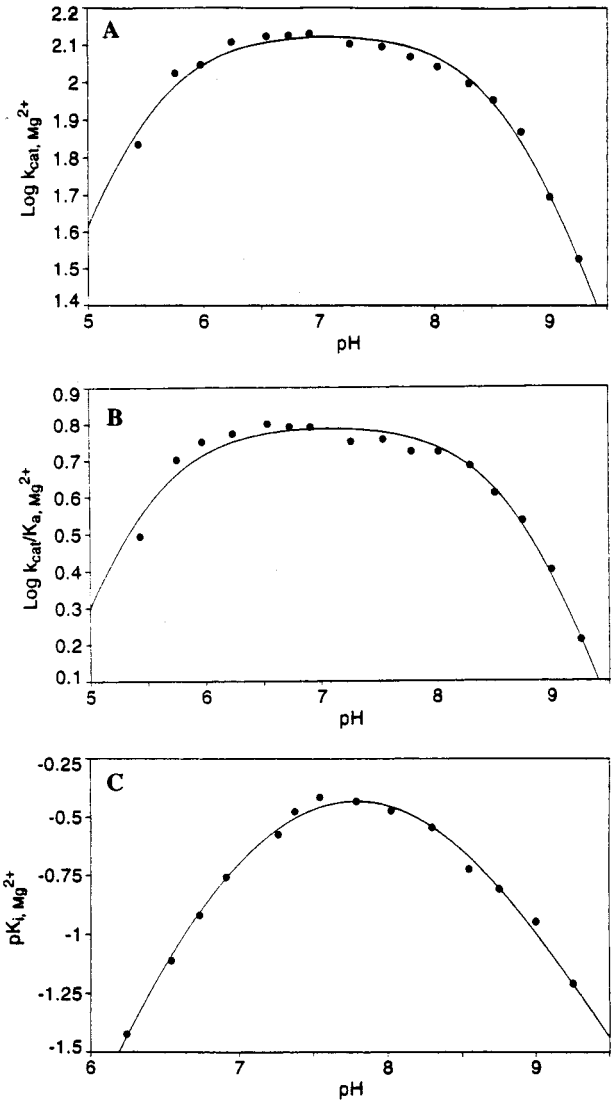

FIGURE 4: The pH effects on the steady-state kinetic parameters of yeast enolase with Mg^{2+}. The steady-state kinetic data for Mg^{2+} as a variable and at saturating PGA (2 mM) is plotted. The kinetic data obtained in the pH range 6.4−9.2 were fit to eq 4. The data for k_{cat} and k_{cat}/K_a were fit to eq 6. The K_i value for Mg^{2+} as a function of pH is described by eq 7. The curves represent the best fit of the data to the equations above. (A) Log k_{cat}, vs pH from fits to Mg^{2+} activation; (B) log $k_{cat}/K_{a,Mg^{2+}}$ vs pH; (C) p$K_{i,Mg^{2+}}$ vs pH.

1.90 ± 0.05 mM for the limiting value for $K_{i,app}$. The pK_A values are summarized in Table 3.

pH Effects on the Steady-State Kinetic Parameters with PGA as a Variable. The interaction of PGA with Mg^{2+}-activated yeast enolase was studied as a function of pH. The kinetics were measured at optimal Mg^{2+} concentration prior to inhibition. The apparent K_m and k_{cat} values were determined over the pH range 5.40−9.25. The variation of log k_{cat} with pH yielded a bell-shaped curve (Figure 5A). The data were fit to eq 6. The resulting value for $k_{cat,max}$ was 115.1 ± 4.3 s^{-1}, and the resulting pK_A values for the two ionizable groups are 5.94 ± 0.12 and 8.35 ± 0.06. The variation of pK_m with pH gives rise to a half-bell profile with slopes of +1 and zero (Figure 5c). As the pH is raised, the K_m value drops to a minimum plateau. Fitting the data to eq 5 yielded a pK_A value of 6.27 ± 0.03 for the ionizable group and of 30.1 ± 0.9 μM for the limiting value for $K_{m,app}$. A plot of k_{cat}/K_m versus pH is a bell-shaped curve with limiting slopes of +2 on the acid side and −1 on the alkaline side (Figure 5b). Data fitted to eq 7 gave the pK_A of the basic group of 8.39 ± 0.08, which is identical to the pK_A value of the basic group in Figure 5A. The acidic portion of the curve yielded the pK_A values of 5.85 ± 0.25 and 6.25 ± 0.15. The equivalence of two pK_A values from Figure 5, panels A and B (except the pK_A of 6.25 ± 0.15), is expected since the $K_{m,app}$ of PGA is invariant in the pH region 6.70−9.25. The results are summarized in Table 3.

The pH dependence of K_m, k_{cat} and k_{cat}/K_m with PGA as the variable was also studied in the presence of inhibitory concentrations of Mg^{2+} (in the pH range of 5.5−9.2 the concentration of Mg^{2+} was varied according to $K_{i,Mg^{2+}}$ to ensure inhibitory conditions). The results and the best fit of the experimental data to the eqs 5−7 is shown in Figure 6. The calculated pK_A values are summarized in Table 3.

DISCUSSION

Investigations have been made into the role played by ionizing residues in the chemical mechanism of the reaction catalyzed by yeast enolase. ^{31}P NMR has been used to identify the ionization state of the enzyme-bound substrates. The investigations have involved determination of the two fundamental kinetic parameters associated with the reaction and of the inhibition constant for the substrate as a function of pH.

The ^{31}P resonances of PGA and PEP bound to the enolase−Mg complex are individually observed by high-field NMR at 202.4 MHz. This indicates that the exchange between PGA and PEP on the enzyme is slow on this time scale (>3 ms). A pH dependence of the ^{31}P chemical shifts gives pK_A values of 5.85 and 6.16 for bound PGA and PEP, respectively, indicating that both ligands preferably bind as the trianionic species (dianionic phosphate and the carboxylate) at neutral pH. Enzyme-bound PGA and PEP are characterized by a change in shielding for both PGA and PEP when bound to enolase−Mg^{2+}. The larger changes in chemical shift with PEP suggest that effects by C−O−P bond angle distortion are greater for bound PEP than for PGA. These chemical shift effects are greater than those for P_i where only ionic and hydrophobic shielding effects would be of importance. Ionic effects on alteration in pK_A values also differ in complexes with PGA and PEP compared to P_i, which is much more symmetrical. The pH effects of the chemical shift for bound PGA and PEP (Figure 3, panels C and D) and the pH effects on the apparent K_m for PGA with a pK_A value of 6.27 ± 0.03 (Figure 5C) and a similar pK_A value in the k_{cat}/K_m (Figure 5B) profile are all due to a single ionization. This pK_A value is consistent with the trianion of PGA preferably binding to the enzyme.

The k_{cat}/K_m and k_{cat} profiles as a function of pH indicate the effect of ionization on binding as well as on catalysis (*24*, *25*). The k_{cat}/K_m profile yields pK_A values of groups on the free enzyme or free substrate and often gives the correct pK_A values. With Mg^{2+} as a variable activator, the same pK_A values (5.9 and 8.4) are seen in both k_{cat} and k_{cat}/K_m profiles. The fraction of the collision complex that reacts to give products, as opposed to dissociation, is the factor responsible for such behavior. Both profiles reflect the ionizations of groups responsible for catalysis since the K_a for Mg^{2+} is invariant in the pH region 5.4−9.25. Similar

Table 3: pH Effects on the Steady-State Kinetic Parameters for Mg^{2+} and for PGA with Yeast Enolase

	$K_{m,PGA}$	$k_{cat,PGA}$	$k_{cat}/K_{m,PGA}$	$k_{cat,Mg^{2+}}$	$k_{cat}/K_{a,Mg^{2+}}$	$K_{i,Mg^{2+}}$
yeast enolase (optimal $[Mg^{2+}]$)	$pK_1 = 6.27 \pm 0.03$[a]	$pK_1 = 5.94 \pm 0.12$[a] $pK_2 = 8.35 \pm 0.06$	$pK_1 = 5.85 \pm 0.25$[a] $pK_2 = 6.25 \pm 0.15$ $pK_3 = 8.39 \pm 0.08$	$pK_1 = 5.84 \pm 0.06$[b] $pK_2 = 8.55 \pm 0.03$	$pK_1 = 5.93 \pm 0.06$[b] $pK_2 = 8.39 \pm 0.03$	$pK_1 = 5.95 \pm 0.20$[b] $pK_2 = 7.13 \pm 0.08$ $pK_3 = 8.35 \pm 0.05$
yeast enolase (inhibitory $[Mg^{2+}]$)	$pK_1 = 6.20 \pm 0.05$[c]	$pK_1 = 6.36 \pm 0.08$[c] $pK_2 = 8.45 \pm 0.03$	$pK_1 = 6.20 \pm 0.08$[c] $pK_2 = 6.35 \pm 0.06$ $pK_3 = 8.49 \pm 0.04$			

[a] Measured with PGA as the variable substrate and Mg^{2+} saturated at 1 mM. [b] Measured with Mg^{2+} as the variable substrate and 2-PGA saturated at 2 mM. [c] Measured with PGA as the variable substrate and $[Mg^{2+}]$ between 1 and 25 mM based on $K_{i,Mg^{2+}}$.

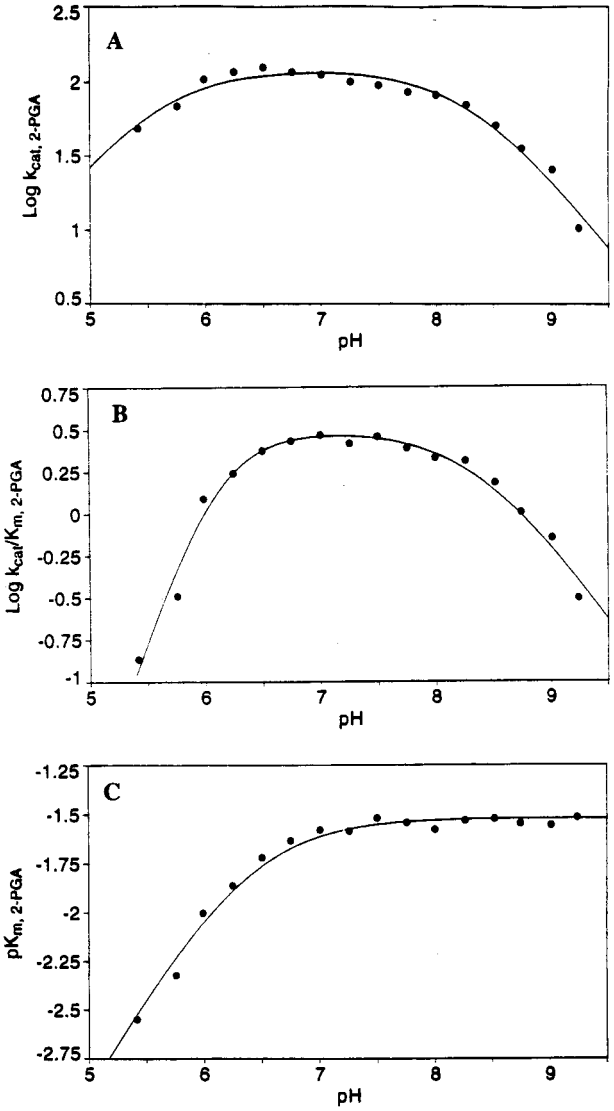

FIGURE 5: The pH effects on the steady-state kinetic parameters for yeast enolase with PGA. The steady-state kinetic data for PGA as a variable and Mg^{2+} concentrations that were optimal prior to the onset of the cation inhibition (1 mM) is plotted. The data for k_{cat} were fit to eq 6. The change in the K_m values of PGA as a function of pH is described by eq 5. The data for k_{cat}/K_m were fitted with eq 7. The curves represent the best-fit of the data to the equations above. (A) log k_{cat} vs pH from fits to PGA activation; (B) log $k_{cat}/K_{m,PGA}$ vs pH; (C) $pK_{m,PGA}$ vs pH.

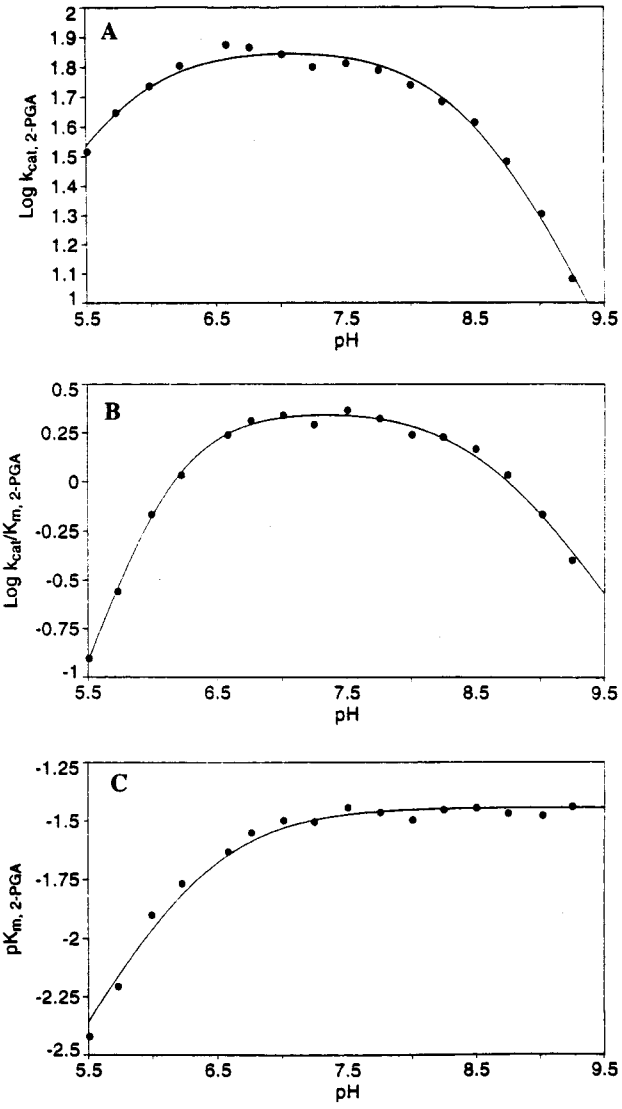

FIGURE 6: The pH effects on the steady-state kinetic parameters for PGA as the variable in the presence of inhibitory concentrations of Mg^{2+}. The steady-state kinetic data for PGA as a variable and inhibitory Mg^{2+} concentrations are plotted. The concentration of Mg^{2+} was varied between 2 and 25 mM depending upon the K_i value. The data for k_{cat} were fit to eq 6. The change in the K_m values of PGA as a function of pH is described by eq 5. The data for k_{cat}/K_m were fit with eq 7. The curves represent the best fit of the data to the equations above. (A) log k_{cat} vs pH from fits to PGA activation; (B) log $k_{cat}/K_{m,PGA}$ vs pH; (C) $pK_{m,PGA}$ vs pH.

pK_A values (5.9 and 8.4) were obtained from k_{cat} and k_{cat}/K_m values with PGA as the variable. These ionizations most likely belong to groups on the enzyme. Since the pK_A values seen in the pH profiles could have contributions from more than one group on the enzyme and/or substrate or could be due to more general effects (global effects such as conformational change), caution should be taken in interpreting the results of the pH study. Nevertheless, an initial guess as to the nature of the residues indicated by the pH profiles could be made. It appears that, for optimal catalysis by yeast enolase, a group with a pK_A of approximately 6.0 must be deprotonated and a group with a pK_A of about 8.5 must be

protonated. The most obvious choices for the groups with pK_A values of approximately 6.0 and 8.5 are a histidine and a lysine, respectively.

The K_m for PGA is pH dependent and a single ionization with a pK_A value of 6.27 is seen in the pK_m profile. The same pK_A is seen in the k_{cat}/K_m profile. When binding occurs by a substrate in a single protonation state, the corresponding pK_A does not appear in the k_{cat} profile (this is common for phosphate esters, many of which bind only as the phosphate dianions). The pK_A value of 6.27 was assigned to the phosphate group of free PGA (vidae supra). Since this ionization is not seen in the k_{cat}/K_m profile for Mg^{2+} as a variable substrate, the pK_A of about 6.27 can be attributed to the group responsible solely for PGA binding. On the basis of the results shown above, it can be concluded that the pH dependence of the kinetic parameters (K_m, k_{cat} and k_{cat}/K_m) for Mg^{2+} and PGA investigated in this study (Table 3) does not support a catalytic function for the phosphoryl group of the substrate. In the initial hypothesis proposed by Nowak et al. (*8*) and modified by Brewer (*16*), the phosphate of PEP was proposed as serving as a base to deprotonate the nucleophilic water bound to the metal ion at site I. The phosphate would serve in the microscopic reverse function from PGA to PEP. This putative function of the phosphate group does not occur.

Yeast enolase binds up to 3 mol of divalent metal ion/subunit in the presence of substrate at neutral pH (*10*). The suggestion that there are all oxygen-containing ligands to the metals at sites I and II is consistent with published crystal structures that showed Asp246, Glu295, and Asp320 to be the ligands to metal ion at site I (*11, 15, 26, 27, 28*). The EPR spectroscopic data of the enolase−Cu complex shows no *g*-factors indicative of N−Cu or S−Cu coupling (*29*). In ^{113}Cd(II) NMR studies, the observed δ is consistent with Cd complexed with oxygen ligands (*30*). Interest is also in the third, inhibitory, metal binding site. Lee and Nowak (*10*) reported that this site appears to be titrated at a pH range of about 6.5−7.0 and may be located either at a histidine-containing site, at the phosphoryl group of the substrate, or at both. Activation studies with Mg^{2+} in the present study show a pH-independent activation (K_a) but a pH-dependent inhibition at higher concentrations of Mg^{2+}. The pH dependence of the K_i (Figure 4C) gives fits with pK_A values 5.95 ± 0.20, 7.13 ± 0.08, and 8.35 ± 0.05. In general, profiles of pK_i detect only groups whose protonation state affects binding. A group with a pK_A from the pK_i profile may or may not act as an acid−base catalyst in the reaction, but its state of protonation clearly affects binding. Specifically, the pK_i profiles for metal activators provide evidence concerning the ligands to the metal (*25*). The pK_A values of these ligands could be perturbed by 1−1.5 pH units by coordination with the metal, and pK_A values would appear in the pK_i profiles. The pK_A values for carboxyls are too low to observe. In the pH profile of pK_i, a break in the curve and a drop in pK_i is expected when a group on either the enzyme or the inhibitor molecule binding to it must be in a specific ionization state for binding to occur. If the improper state of ionization leads to no binding, the profile changes to a line with a slope of +1 when protonation prevents binding or −1 when deprotonation prevents binding. The breaks occur at the true pK_A values of the ionizing groups. The binding of Mg^{2+} is prevented when a group with a pK_A of 8.35 is deprotonated or when a group with a pK_A of 5.95 and a group with a pK_A of 7.13 become protonated (Figure 4C). Since none of these pK_A values could be attributed to Mg^{2+}, they must represent groups on the enzyme and/or substrate, PGA. The pK_A value of 5.95 could be attributed to the phosphate group of the enzyme-bound PGA. A similar pK_A value (5.85) was obtained for the phosphate group of enzyme-bound substrate in the ^{31}P-NMR titration experiment. The pK_A on the basic side of the profile could be attributed to a metal-bound water molecule that can act as a neutral acid with pK_A about 8.3. Alternatively, the pK_A = 8.3 may be the same residue involved in k_{cat} and in $k_{cat}/K_{m,PGA}$ required for formation of the catalytically active ternary (E−M−S) complex and catalysis. The pK_A of 7.13 might be attributed to the histidine at the active site.

If a histidine residue is the catalytic base in yeast enolase, it abstracts the C-2 proton in the initial step of the reaction. Binding of a metal ion at site three interferes with the initial step of the reaction. When Mg^{2+} binds at site III, the cation can interect with a His. An alteration of His159 at the catalytic site occurs resulting in a perturbation of the active-site base possibly by changing its environment and/or conformation resulting in a shift in pK_A from 5.9 to 6.4 (Table 3). The pK_A on the basic side of the pH curve remains unchanged (Table 3). On the basis of the above analysis, it appears that potential ligands to the third, inhibitory, metal site on yeast enolase could be a histidine residue, the phosphate group of PGA, and one or several water molecules. This proposal is consistent with such a catalytic mechanism of yeast enolase. Binding of metal ion at site III alters the histidine residue making it a less efficient catalytic base to abstract the C-2 proton of PGA.

Poyner et al. (*31*) have proposed that Glu211−Lys345 is the general acid−base pair in the enolase reaction. The results of the present study argue against this proposal. On the basis of the pK_A values obtained from k_{cat} and k_{cat}/K_m results with Mg^{2+} and PGA as variables, it appears that an unprotonated residue with a pK_A of about 6.0 and a protonated residue with a pK_A of about 8.4 are important for substrate binding and catalysis and these are unlikely to be Lys (pK_A = 6.0) and Glu (pK_A = 8.4) residues, respectively.

In the Mn^{2+}−phosphoglycolate complex of lobster enolase (*14*), the imidazole group of His157 (His159 in the yeast enolase numbering system), is in van der Waals contact (4.5 Å) with the C-2 atom of the inhibitor. This position is the consequence of a movement of loop L2 toward the inhibitor. In the apoenzyme, loop L2 is disordered, and there is no interpretable density for its side chains. The position of loop L2 in this particular ternary complex was also observed by Lebioda et al. (*15*) in a complex of yeast enolase with phosphate and fluoride but not with substrate analogues. In the phosphonoacetohydroxamate−Mg^{2+} complex (*27*), the equivalent His159 is in contact with the inhibitor and interacts with the phosphonate. Thus, at least two X-ray structures of yeast enzyme confirm that loop L2 can move to a position where the histidine is at the active site. From the crystal structure by Duquerroy et al. (*14*), it appears that Lys396, located by the C_3−OH, is capable of donating a proton to the leaving hydroxyl group. Furthermore, His159 and Lys396 are located on the opposite sides of the substrate

as seen in several crystal structures (*11*, *14*, *15*). We would like to suggest that Lys396−His159 is the catalytic acid−base pair in yeast enolase. Lysine is less frequently used as a base with pK_A = 5.9 in enzymatic catalysis but can serve as a proton donor with a pK_A = 8.4.

In summary, the results presented in this paper do not support a catalytic function for the phosphoryl group of the substrate and demonstrate that an unprotonated His and a protonated Lys are important for substrate binding and catalysis. Lys396 and His159 are proposed to be the catalytic acid−base pair in yeast enolase. Furthermore, His159 and the phosphate group of the enzyme-bound substrate appear to be at the inhibitory metal site III. Binding of metal ion at site III inhibits enzymatic activity by interfering with the first step of the reaction, proton abstraction.

ACKNOWLEDGMENT

The authors would like to thank Don Schifferl for help in setting up the NMR experiments and Mike Buening for helpful discussions regarding these studies.

REFERENCES

1. Brewer, J. M., and Weber, G. (1966) *J. Biol. Chem. 241*, 2550−2557.
2. Brewer, J. M. (1981) *CRC Crit. Rev. Biochem. 9*, 209−254.
3. Chin, C. C. Q., Brewer, J. M., and Wold, F. (1981) *J. Biol. Chem. 256*, 1377−1384.
4. Wold, F., and Ballou, C. (1957) *J. Biol. Chem. 227*, 301−312.
5. Cohn, M., Pearson, J. E., and Rose, I. A. (1970) *J. Am. Chem. Soc. 92*, 4095−4102.
6. Dinovo, E. C., and Boyer, P. D. (1971) *J. Biol. Chem. 246*, 4586−4593.
7. Shen, T. Y. S., and Westhead, E. W. (1973) *Biochemistry 12*, 3333−3337.
8. Nowak, T., Mildvan, A. S., and Kenyon, G. L. (1973) *Biochemistry 12*, 1690−1701.
9. Hanlon, D. P., and Westhead, E. W. (1969) *Biochemistry 8*, 4247−4255.
10. Lee, B. H., and Nowak, T. (1992) *Biochemistry 31*, 2165−2171.
11. Larsen, T. M., Reed, G. H., Wedekind, J. E., and Rayment, I. (1996) *Biochemistry 35*, 4349−4358.
12. Lebioda, L., and Stec, B. (1991) *Biochemistry 30*, 2817−2822.
13. Poyner, R. R., Reed, G. H., Laughlin, L. T., and Sowa, G. A. (1996) *Biochemistry 35*, 1692−1699.
14. Duquerroy, S., Camus, C., and Janin, J. (1995) *Biochemistry 34*, 12513−12523.
15. Lebioda, L., Zhang, E., Lewinski, K., and Brewer, J. M. (1993) *The Proteins 16*, 219−225.
16. Brewer, J. M. (1985) *FEBS Lett. 182*, 8−14.
17. Warburg, O., and Christian, W. (1941) *Biochemistry Z. 310*, 384−421.
18. Nowak, T., and Maurer, P. J. (1981) *Biochemistry 20*, 6890−6911.
19. Lee, M. E., and Nowak, T. (1992) *Biochemistry 31*, 2172−2180.
20. Westhead, E. W. (1966) *Methods Enzymol. 9*, 670−679.
21. Westhead, E. W., and McLaine, G. (1964) *J. Biol. Chem. 239*, 2464−2468.
22. Wüthrich, K., Schick, M., Betz, A., and Stone, S. R. (1994) *Biochemistry 33*, 9303−9310.
23. Perella, F. W. (1988) *Anal. Biochem. 174*, 437−441.
24. Cleland, W. W. (1982) *Methods Enzymol. 87*, 390−405.
25. Tipton, K. F., and Dixon, H. B. F. (1979) *Methods Enzymol. 63*, 183−233.
26. Lebioda, L., and Stec, B. (1989) *J. Biol. Chem. 264*, 3685−3693.
27. Wedekind, J. E., Reed, G. H., Poyner, R. R., and Rayment, I. (1994) *Biochemistry 33*, 9333−9342.
28. Zhang, E., Lebioda, L., and Brewer, J. M. (1994) *Biochemistry 33*, 6295−6300.
29. Dickinson, C. C., Rose, S. L., and Westhead, E. W. (1980) *J. Inorg. Biochem. 13*, 323−366.
30. Spencer, S. G., Brewer, J. M., and Ellis, P. D. (1985) *J. Inorg. Biochem. 24*, 47−57.
31. Poyner, R. R., and Reed, G. H. (1992) *Biochemistry 31*, 7166−7173.

BI981047O